Study on the Adsorption of Heavy Metal Ions from Aqueous Solution on Modified SBA-15

Liliana Giraldo[a], *Juan Carlos Moreno-Piraján*[b]*

[a]*Facultad de Ciencias, Universidad Nacional de Colombia, Bogotá, Colombia*
[b]*Grupo de Investigación en Sólidos Porosos y Calorimetría, Facultad de Ciencias,*
Universidad Nacional de Colombia, Bogotá, Colombia

Amino-functionalized SBA-15 mesoporous silica was prepared, characterized, and used as an adsorbent for heavy metal ions. The organic–inorganic hybrid material was obtained by a grafting procedure using SBA-15 silica with 3-aminopropyl-triethoxysilane and bis(2,4,4-trimethylpentyl) phosphinic acid (Cyanex 272), respectively. The structure and physicochemical properties of the materials were characterized by means of elemental analysis, X-ray diffraction (XRD), nitrogen adsorption–desorption, thermogravimetric analysis, FTIR spectroscopy and immersion calorimetry. The organic functional groups were successfully grafted onto the SBA-15 surface and the ordering of the support was not affected by the chemical modification. The behavior of the grafted solids was investigated for the adsorption of heavy metal ions from aqueous solutions. The hybrid materials showed high adsorption capacity and high selectivity for zinc ions. Other ions, such as cooper and cobalt were absorbed by the modified SBA-15 material.

Keywords: *SBA-15, isotherms, heavy ions, immersion calorimetry, FTIR*

1. Introduction

A wide variety of toxic inorganic and organic chemicals are discharged into the environment as industrial wastes, causing serious water, air, and soil pollution. Heavy metals are found in wastewaters originating from chemical manufacturing, painting and coating, mining, extractive metallurgy, nuclear, and other industries[1,2]. The most abundant harmful metals in liquid effluents are Cr, Ni, Zn, Cu, and Cd. They are considered persistent, bioaccumulative and toxic substances. Such metals exert a deleterious effect on the fauna and flora of lakes and streams. One of the potential remedies to this problem is the use of adsorption technologies. Activated carbons[3] and a number of low-cost adsorbents such as agricultural residues and peat[4-7] have been used for the removal of heavy metal cations. However, the major disadvantages of these adsorbents are their low loading capacities and their relatively weak interactions with metallic cations, as evidenced by low metal ion binding constants[8,9]. To overcome this drawback, many investigators have developed functionalized adsorbents such as organoclays and surface-modified mesoporous materials. In the case of natural clays, quaternary ammonium compounds and/or thiols have been used to modify clays such as smectite and montmorillonite[1,10-13]. Mesoporous silicas, such as MCM-41[14-19], HMS[20,21], SBA-15[22], and SBA-11[7] have been functionalized by various groups to afford materials able to interact strongly with metallic cations, particularly mercury[14-16,20-22] or metallic anions such as chromate and arsenate[17-19]. Porous silica functionalized with various chelating agents is increasingly utilized as

an adsorbent because of its high selectivity for metal ion adsorption[23-26]. The discovery of hexagonally ordered mesoporous silicas[27] has stimulated renewed interest in adsorbent and catalyst design because of their unique large surface area, well-defined pore size and pore shape. The addition of organic groups by the grafting of organosiloxane precursors onto the surface of the pores results in functional mesoporous hybrid materials[28-36]. These organic–inorganic hybrid materials have been reported to exhibit improved sorption properties toward heavy metal ions, superior to those achieved with silica gel functionalized with the same ligand[37,38]. Unfortunately, the most extensively investigated mesoporous material, MCM-41 silica, shows low mechanical and hydrothermal stability. It has been shown that the low hydrothermal stability of the MCM-41 material is due to the hydrolysis of its thin (1-2 nm thickness) pore walls[39,40]. In 1998, Zhao et al. (1998) developed SBA-15 mesostructured silica, which consists of parallel cylindrical pores with the axes arranged in a hexagonal unit cell. SBA-15 usually has wider pores than MCM-41 (SBA-15 pores range from 5 to 30 nm in diameter), and higher pore volumes. Moreover, in comparison with other mesostructured silica materials, SBA-15 exhibits thicker pore walls (between 3.1 and 6.4 nm thick) which provide high hydrothermal stability[41,42], and render the material suitable for use in aqueous media. SBA-15 surface modifications with organic species for adsorption applications have been presented. Functional groups, such as thiol[43,44], imidazole[45], amino[37,46], polyol[47], and iminodiacetic acid[48] have been incorporated into the inorganic SBA-15 network. Thiol-functionalized SBA-15

*e-mail: jumoreno@uniandes.edu.co

silicas have exceptional selectivity for adsorbing $Hg^{2+[37,44]}$ and noble metals[43] from waste streams. Imidazole-derivatized SBA-15 exhibit a high adsorption capacity for Cr (VI)[45]. Amino-functionalized SBA-15 show a high affinity for different metal ions, such as Cu^{2+}, Zn^{2+}, Cr^{3+} and $Ni^{2+[46]}$. A report in the literature[7] has shown that SBA-15 with polyol functional groups possesses very good boron adsorption capacity. Very recently[48], iminodiacetic acid-modified SBA-15 hybrid material has demonstrated an excellent ability to remove Cd^{2+} from aqueous solutions. Schiff base-type groups, easily prepared by condensation between aldehydes and amines, are known as very efficient chelating agents for many different metals[49].

The present study had two aims. Firstly, we synthesized and characterized a new hybrid material, i.e., SBA-15 mesoporous silica modified with 3-aminopropyl-triethoxysilane and bis(2,4,4-trimethylpentyl) phosphinic acid (Cyanex 272). Secondly, we studied the applicability of this material for the removal of heavy metal ions from aqueous solutions and, through the heats of immersion of each of the ions under study, we established the relationship between the modification of SBA and immersion enthalpy.

2. Experimental

2.1. *Preparation of functionalized SBA-15 silica*

SBA-15 material was synthesized as described in[41]. The organic–inorganic hybrid materials were obtained by a grafting procedure with 3-aminopropyl-triethoxysilane and bis(2,4,4-trimethylpentyl) phosphinic acid (Cyanex 272), respectively. Firstly, the calcined SBA-15 was silanized with 3-aminopropyl-triethoxysilane adapted according to a previously described procedure[50,51]. One gram of SBA-15 silica, freshly activated overnight at 506 K under vacuum, and 2.7 mL of 3-aminopropyl-triethoxysilane (99% Aldrich) were added to 85 mL of dry toluene. After stirring the solution (reflux, 12 hours), the released ethanol was distilled off and the mixture was kept under reflux for 220 minutes. The NH_2-functionalized mesoporous silica (referred as NH_2–SBA-15) was filtered and washed with toluene, ethanol, and diethyl ether. It was then submitted to a continuous extraction run overnight in a Soxhlet apparatus using diethyl ether/dichloromethane (v/v, 1/1) at 450 K and dried overnight at 430 K. On the other hand, industrial-grade Cyanex 272 was purified using a published procedure[52] in which 12.0 g of SBA-15 were contacted with 80 mL of a 1:1 mixture of purified Cyanex 272 and toluene in a screwcap bottle at 340 K for 48 hours. The Cyanex 272-loaded SBA-15 was washed with distilled water and filtered using a Millipore apparatus. The filtered CY-SBA was then dried at room temperature under vacuum overnight. These two hybrid materials are referred to as NH_2–SBA and CY-SBA-15, respectively.

2.2. *Characterization*

Small-angle XRD data were acquired on a Bruker diffractometer using Cu Kα radiation. N_2 adsorption–desorption isotherms were measured at 77 K with a Quantachrome Autosorb 3B (Boynton Beach, FL, USA).

The samples were degassed at 323 K for 12 hours prior to the adsorption measurements. Specific surface area was calculated by the BET method, the mesopore volume was determined by nitrogen adsorption at the end of capillary condensation, and the pore size distribution was determined from the desorption isotherms using the Barrett-Jonyner-Halenda (BJH) method. The FTIR spectra of self-supported wafers previously heated at 423 K under vacuum were performed on a Bruker Vector 22 spectrometer. Atomic absorption spectrophotometry (FAAS) measurements were performed on a Spectra AA-220 Varian spectrophotometer equipped with Varian multi-element hollow cathode lamps and air–acetylene burner. The C, H, and N contents were evaluated by combustion on a 1108 FISON CE analyzer (Italy) elemental analysis apparatus.

The SBA-15 studies were carried out in the TGA Netzsch STA-409C, in which SBA-15 was placed in an alumina crucible and heated from room temperature up to 1200 °C using a flow of nitrogen at 100 mL/min, with a heating rate of 5 °C/min. An empty pure alumina crucible served as an inert reference.

2.3. *Metal ion adsorption tests*

Analytical grade cobalt (II) nitrate $(Co(NO_3)_2)$, copper(II) nitrate $(Cu(NO_3)_2.5H_2O)$, and zinc nitrate $Zn(NO_3)_2$ from J.T. Baker were used in the experiments without further purification. Stock solutions of metal ions were prepared using deionized water Adsorption tests were carried out at room temperature, under batch conditions, by mixing the adsorbent with the aqueous solutions at pH 4.8 (0.1 M phthalate buffer solution), under stirring (100 rpm). After 60 minutes, the adsorbent was filtered and the residual metal concentration in the solution was measured by atomic absorption spectrophotometry. Ion competitive adsorption studies were performed by treating 100 mL of a mixed metal solution containing equimolar amounts (100 mmol L^{-1} of Co^{2+}, Cu^{2+}, and Zn^{2+} ions) with 100 mg of the adsorbent for 60 minutes, under stirring, at room temperature. For all adsorption tests, the deviation between the initial and final pH was less than 0.1 pH units.

2.4. *Adsorption equilibrium isotherm*

Batch sorption experiments were conducted using 100 mL aliquots of the test solution containing 100 mg.L^{-1} of each one of the ions: Co^{2+}, Cu, and Zn^{2+} with the pH adjusted between acid (approximately pH 4.8) and placed in 250 mL amber closed bottles. Later, known quantities (0.01-0.15 g) of modified SBA-15 were added to each bottle and the pH was adjusted using either 0.1 M nitric acid or 0.1 M sodium hydroxide. The solutions were stirred at 250 rpm for 5-120 minutes at 25 ± 1 °C. The modified SBA-15 was removed by filtration and the Co^{2+}, Cu^{2+}, and Zn^{2+} contents of the filtrate were measured by atomic absorption spectroscopy (AAS). Percent removal (R %) was calculated according to the following equation:

$$R = \frac{C_0 - C_e}{C_0} 100 \qquad (1)$$

where R is the percent removal of Co^{2+}, Cu^{2+}, and Zn^{2+}, C_0 and C_e are the initial and residual concentrations (mg.L^{-1}) of Co^{2+}, Cu^{2+}, and Zn^{2+}, respectively. Adsorption isotherms were obtained with different initial concentrations of Co^{2+}, Cu^{2+}, and Zn^{2+} while maintaining the modified SBA-15 dosage at a constant level. Control determinations were carried out in the absence of modified SBA-15 in order to correct for any adsorption of Co^{2+}, Cu^{2+} and Zn^{2+} on the container surface. These experiments indicated that no adsorption by the container walls occurred. In all experiments, the difference between the initial Co^{2+}, Cu^{2+}, and Zn^{2+} concentration (C_0) and the equilibrium concentration (C_e) was calculated and used to determine the adsorptive capacity (q_e) as follows:

$$q_e = \frac{V}{m}(C_0 - C_e) \qquad (2)$$

where V is the total volume of Co^{2+}, Cu^{2+}, and Zn^{2+} solution (mL), m is the mass of adsorbent used (g), C_0 is the initial concentration of Co^{2+}, Cu^{2+}, and Zn^{2+} solutions (mg.L^{-1}), and C_e is the residual Co^{2+}, Cu^{2+}, and Zn^{2+} concentration (mg.L^{-1}). The linear model, which describes the accumulation of the solute by the sorbent as directly proportional to the solution concentration is presented by the relation:

$$q_e = K_D C_e \qquad (3)$$

The proportionality constant or distribution coefficient K_D is often referred to as the partition coefficient. The Langmuir model represents one of the first theoretical treatments of non-linear sorption, and has been successfully applied to a wide range of systems that exhibit limiting or maximum sorption capacities. The model assumes uniform energies of adsorption onto the surface and no transmigration of the adsorbate on the plane of the surface.

The Langmuir isotherm is given by:

$$q_e = \frac{Q^o b C_e}{1 + b C_e} \qquad (4)$$

where Q^o and b are Langmuir constants related to the adsorption capacity and energy of adsorption, respectively. Equation 4 is usually linearized by inversion to obtain:

$$\frac{1}{q_e} = \frac{1}{Q^o} + \frac{1}{bQ^o}\frac{1}{C_e} \qquad (5)$$

Equation 3 is equally used to analyze batch equilibrium data by plotting $1/q_e$ versus $1/C_e$, which yields a linear plot if the data conform to the Langmuir isotherm.

The Freundlich isotherm is the most widely used non-linear sorption model and is given by the general form:

$$q_e = K_F C_e^{1/n} \qquad (6)$$

where K_F is related to sorption capacity and n to sorption intensity. The logarithmic form of Equation 6) given below is usually used to fit data from batch equilibrium studies:

$$\log q_c = \log K_F + \frac{1}{n}\log C_e \qquad (7)$$

2.5. *Immersion enthalpy*

The immersion enthalpies of SBA-15 were determined in solutions of Co^{2+}, Cu^{2+}, and Zn^{2+} of different concentrations ranging from 20 to 100 mg.L^{-1} for the maximum adsorption of pH 4.8. The immersion enthalpies were also determined for solutions of 100 mg.L^{-1} at all pH values studied. This determination was performed in a heat conduction microcalorimeter with a stainless steel calorimetric cell[52], in which 30 mL of the solution to be used were pre-heated at 298 K, then placed in the cell. A sample of activated carbon of approximately 0.500 g was weighed and placed inside the calorimetric cell in a glass ampoule. The microcalorimeter was then assembled. When the equipment reached a temperature of about 298 K, the potential readings were registered after a period of approximately 15 minutes, with readings every 20 seconds once the glass ampoule was broken and the thermal effect registered. Potential readings continued for approximately another 15 minutes and, at the end of the experiment, the equipment was electrically calibrated.

3. Results and Discussion

3.1. *Physicochemical properties of SBA-15 and modified SBA-15 materials*

The organic functional groups were synthesized by grafting on the SBA-15 surface by a step synthesis procedure (Figure 1). The surface hydroxyl groups were reacted with the ethoxy groups of aminopropyl triethoxysilane and bis (2, 4, 4-trimethylpentyl) phosphinic acid. Based on the elemental and thermogravimetric analysis, the amount and the density of the functional groups grafted on the SBA-15 surface were measured. Thus, the amounts of grafted aminopropyl and Cyanex 272 groups per nm^2 (of pure SBA-15 silica) were 3.2 and 2.7, respectively. As previously reported in the literature, the average number of silanol groups (quantified by ^{29}Si NMR spectroscopy) for the SBA-15 material is 3.6 OH nm^2[53]. Based on this density of silanol groups, the calculated yield of the aminopropyl grafting was about 82%. The Cyanex 272 coupling reaction onto SBA-15 was more efficient that with aminopropyl; the chemical process of the functionalized area is described in Figure 1.

From the elemental analysis data, it was also established that the C/N and H/N atom ratios in the NH$_2$–SBA-15 sample were 7.0 and 18.2, respectively. This result suggests that the stoichiometry between the silanol group and the silylating agent was 1:1, indicating that most of the aminopropyl silane chains were linked to the pore wall surface only by one Si–O–Si bond (Figure 1), a result found by others authors[54]. The C/N molar ratio calculated for the CY–SBA-15 sample was 15.7, indicating a 1:1.5 stoichiometry between the phosphinic group and SBA-15. Thus, the amount of phosphinic groups grafted on this material was 2.0 molecules nm^2. The XRD measurements (not shown here) confirmed the SBA-15 structure for both unmodified and grafted samples. The SBA-15 material exhibited a strong (100) reflection peak (at $2\theta = 0.7°$) and smaller (110), (200), (210) diffraction peaks, which are characteristic of a well-ordered SBA-15 type material[55]. No significant changes were observed upon amine

immobilization, except for the expected decrease in XRD peak intensity, providing evidence that functionalization occurred mainly inside the mesopore channels. However, CY-SBA-15 had some slight differences which were more marked due to the structure of Cyanex 272, which when coupled to the SBA-15 left a group exposed and generated phosphorus peaks at angles of 20°.

All materials exhibited irreversible type IV adsorption–desorption isotherms (Figure 2) with an H1 hysteresis loop in the partial pressure range from 0.65 to 0.75, characteristic of materials with a pore diameter of 7-8 nm. This result reveals that the uniform mesoporous nature of the material was preserved even though grafting had occurred.

The main textural properties of the solids are listed in Table 1. We noted that for the functionalized SBA-15 materials, the BET surface and volume were standardized versus pure silica weights. As expected, the BET surface area and the mesopore volume strongly decreased after

grafting, according to the sequence SBA-15 > NH_2–SBA-15 > CY-SBA-15. These results are in agreement with other authors[54].

For example, for the aminopropyl functionalized mesoporous silica (NH_2–SBA-15) and CY-SBA-15, the BET surface area and the mesopore volume were diminished by 61% and 51, respectively, comparatively to the SBA-15 support. These textural results confirm that the grafted species were located inside the mesopores and not only on the outer surface[54].

Table 1. Textural properties of modified SBA-15 materials synthesized by grafting.

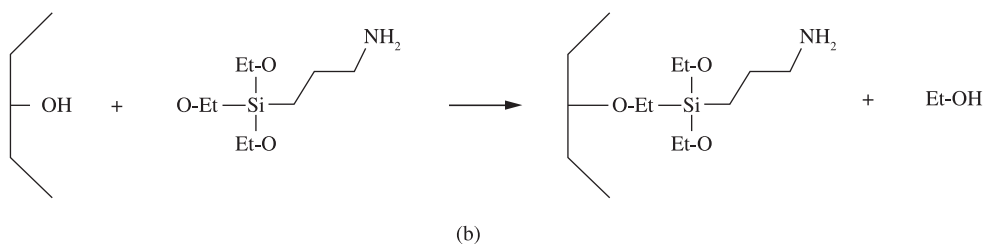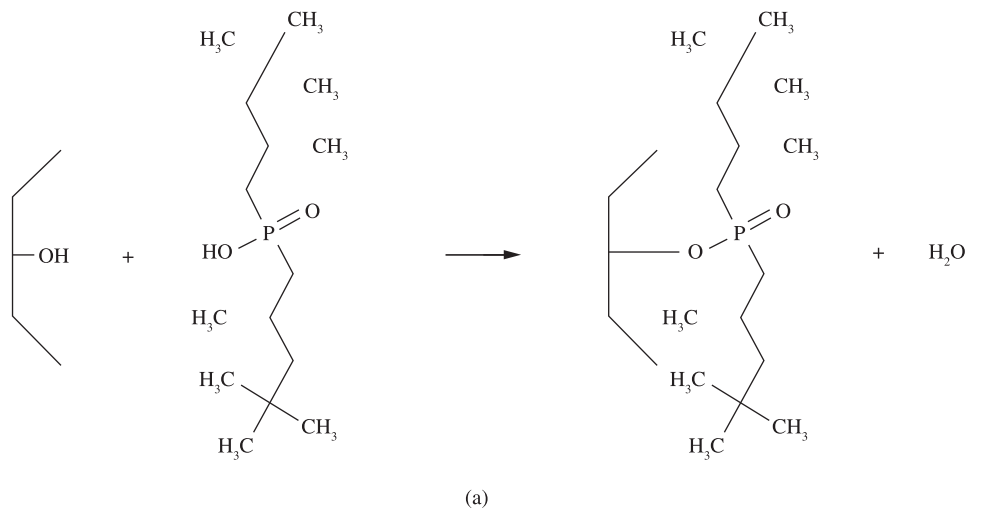| Sample	SBET (m2g-1)	Vmeso (mL.g-1)	D (nm)
SBA-15	565	1,24	7,8
NH2-SBA-15	345	0,86	6,5
CY-SBA-15	287	0,49	5,6

(a)

(b)

Figure 1. Schematic illustration of SBA-15 functionalization.
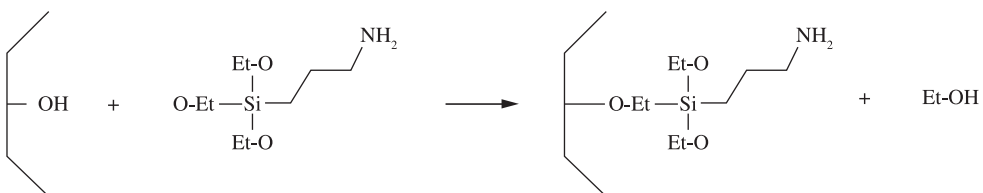

Figure 2. Nitrogen adsorption-desorption isotherm at 77 K of SBA-15 and modified SBA-15.

The FTIR spectra of the SBA-15 precursor and organic–inorganic hybrid SBA-15 materials previously heated at 423 K under vacuum were assessed. At this temperature, only the physisorbed water was removed from the samples, as was determined from the TGA curves (not shown here). The FTIR spectrum of SBA-15 showed typical bands at 3550-3800 cm^{-1} due to the presence of silanol groups. After functionalization with aminopropyl groups, the intensity of the bands corresponding to these groups decreased with a concomitant increase in the bands characteristic of immobilized aminopropyl groups (NH$_2$–SBA-15 spectrum), indicating that a reaction between the OH groups of the silica network with the ethoxy groups of the organic precursor had taken place. As previously reported[37,46-48], the new bands can be attributed to both symmetric and asymmetric stretching of CH$_3$ and CH$_2$ groups (v_{as} (CH$_3$) = 2950 cm^{-1}, v_{as} (CH$_2$) = 2940 cm^{-1}, v_s ms (CH$_3$) = 2910 cm^{-1}, v_s (CH$_2$) = 2905 cm^{-1}) and of NH$_2$ function (v_{as} = 3500 cm^{-1}, v_s = 3450 cm^{-1}). A band at 1600 cm^{-1} (δN–H) was also identified. These results are very similar to the findings of other authors[54].

These results confirm the successful functionalization of SBA-15 with aminopropyl groups. Characteristic bands can also be observed in the FTIR spectrum of the CY–SBA-15 material (not show here). In the infrared spectrum, the CH-stretching (methyl, methylene) appears as a very strong band at 2970 cm^{-1}, and other v (C–H) stretching (symmetric and anti-symmetric) bands at 2930 and 2880 cm^{-1} are seen. The bonded OH vibration gives bands at 2800 and 2400 cm^{-1}, whereas the very broad bands occurring at 1800-1700 cm^{-1} represent OH deformation. The v (P–O) stretching band for Cyanex-272 is found at 1286 cm^{-1}. The v (P–O) anti-symmetric stretching band appears as a broad band at 1080 and a v (P–O) symmetric stretching band is seen at 786 cm^{-1}. Furthermore, the IR spectrum of modified SBA-15 with Cyanex-272 shows a broad band at 1200-1180 cm^{-1} for C–C–C anti-symmetric stretching. Symmetric and anti-symmetric stretching bands of methyl and methylene C–H occurring in Cyanex-272 at 3000, 2970, and 2900 cm^{-1} are also present in all the metal-Cyanex-272 complexes, as expected (not shown). However, the OH stretching bands appearing at 2800 and 2400 cm^{-1} are missing in all the spectra of the prepared metal Cyanex-272 complexes. This indicates deprotonation of P–OH before complexation, which signifies the normal cation exchange behavior of the ligand Cyanex-272. Therefore, the metal ions are assumed to form strong complexes with the ligand Cyanex-272. In the case of metal-Cyanex-272 complexes, the shifting of v (P–O) vibrational bands occurred at 1300, 1070, and 784 cm^{-1} in pure Cyanex-272. The v (P-O) vibration band at 1286 cm^{-1} shifted towards lower frequencies (1260 cm^{-1}) in all of the Cyanex- 272 complexes. The anti-symmetric v (P–O) stretching band at 1049 cm^{-1} shifted to lower frequencies (1029 cm^{-1}) in the Zn(II)-Cyanex-272-SBA-15 complex, whereas in the Co(II) and Cu(II) complexes, it shifted towards higher frequencies (1085 cm^{-1}).

3.2. *Heavy metal ion adsorption studies*

3.2.1. Evidence of metal ion complexation

Transition metal ions (Cu^{2+}, Zn^{2+}, and Co^{2+}) were incorporated into the functionalized SBA-15 silica by treating this material with solutions containing metal salts. It is known that pH is an important parameter in the ion adsorption process. In order to prevent the precipitation of metallic cations, the solution pH must be adjusted in the range 1.76-6.2[55]. The best adsorption performance was obtained in the pH range of 4-5.5[55,56]. Based on these results, in this study, we performed the adsorption tests at pH 4.8. The resulting Me^{2+}–SBA-15 solids were characterized by FTIR spectroscopy(not show here). In order to establish the nature of the bands of the complexes, the FTIR bands were compared with those of the free ligands. The band assigned to –C≡N stretching vibration of the imine group (which was observed at 1650 cm^{-1} for the free ligand) appeared at lower frequencies in the spectra of Me^{2+}–SBA-15 complexes, indicating the coordination of the imine nitrogen with the Me^{2+} ion[54,57]. This feature can be explained by the withdrawal of electrons from the nitrogen atom to the metal ion. The band assigned to the C–O group (at 1287 cm^{-1} for the free ligand) also shifted to lower frequencies after metal adsorption. The new bands at about 500 and 400 cm^{-1} appearing for the complexes are assigned to the v (Me–O) and (Me–N) vibration modes, respectively.

3.3. *Metal ion adsorption studies*

3.3.1. Adsorption in homoionic solutions.

The amount of metal ions adsorbed by CY–SBA-15 (Q, mg g^{-1}), the distribution coefficient (K$_D$, mL.g^{-1}), and the removal level for each ion are summarized in Table 2. The metal loading capacities of the different

Table 2. Isotherm parameters of Co^{2+}, Cu^{2+}, and Zn^{2+} adsorption on modified SBA-15.

	Langmuir			Freundlich		
	qo(mg/g)	KD (L.mol-1)	R2	KF (L.mmol-1)	n	R2
CY-SBA-15/Zn	169,531	0,053	0,9990	14,192	2,354	0,9885
CY-SBA-15/Cu	139,031	0,029	0,9992	11,141	2,176	0,9903
CY-SBA-15/Co	104,477	0,031	0,9963	7,562	1,896	0,9895
NH2-SBA-15/Zn	147,186	0,017	0,9988	5,028	1,695	0,9924
NH2-SBA-15/Cu	122,162	0,011	0,9971	2,919	1,477	0,9912
NH2-SBA-15/Co	120,201	0,013	0,9948	3,467	1,531	0,9882
SBA-15/Zn	68,932	0,007	0,9926	1,268	1,313	0,9864
SBA-15/Cu	58,952	0,003	0,9946	0,625	1,131	0,9924
SBA-15/Co	47,062	0,001	0,9910	0,209	0,920	0,9936

adsorbents for an initial ion concentration of 100 mg.L^{-1} are included in Table 2. Each value in these tables is the mean of five determinations with an accepted relative standard deviation of ±3%. Based on these results, some remarks can be made: (a) the Q values corresponding to the functionalized CY–SBA-15 and NH$_2$–SBA-15 samples were much larger than those obtained with the unmodified SBA-15 (for this material, the Q values were less than 40.0 mg.g^{-1}), confirming the favorable role played by the functional group used in the modification of SBA-15; (b) the mesostructured CY–SBA-15 material was more efficient than the modified silica gel NH$_2$–SBA-15 samples; (c) the CY–SBA-15 adsorbent showed very good adsorption capacity for the all ions studied, in particular for the zinc ion, which was much higher compared to the other metal ions; (d) the loading capacities decreased in the following order: Zn^{2+} > Cu^{2+} > Co^{2+}. For the maximum loading level of the Zn^{2+}-containing complex (89.0 mg.g^{-1}), the zinc/nitrogen molar ratio was 0.62, which is in agreement with the expected value of 0.5 reported by other authors[54]. This confirms that the functionalization of zinc onto the CY–SBA-15 support proceeded with the intended Zn–SBA-15 complex format in a 1:2 molar ratio (Figure 1). The extent of functional group participation in metal ion complexation for the tested adsorbents was calculated based on the amount of groups grafted on the silicas, considering a metal/ligand ratio of approximately ½. The following amounts of complexed metal ions were determined for modified SBA-15: (a) CY–SBA-15: 94.5 (Zn^{2+}), 75.6 (Cu^{2+}), and 56.3(Co^{2+}) (b) CY–SBA-15: 100 (Zn^{2+}), 61.4 (Cu^{2+}), and 31.8 (Co^{2+}). These results may be related to the formation constants (K$_f$) of the metal ion–ligand complexes. Indeed, according to the Irving–Williams series[58,59], the bond strength between a ligand (despite its nature) and a series of metal cations depends on the K$_f$ parameter. For the metal ions investigated in this study, the K$_f$ values, and implicitly the bond strength between the metal ion and the ligand, increased in the following order: Co^{2+} < Cu^{2+} < Zn^{2+}. Our results are completely in agreement with this rule[54-59].

3.3.2. Adsorption isotherms from aqueous solution

Adsorption data are usually discussed and explained using isotherm adsorption models, such as the linear, Langmuir, and Freundlich isotherms. These isotherms relate metal uptake per unit weight of the adsorbent, q$_e$, to the equilibrium adsorbate concentration in the bulk fluid phase, C$_e$. Equations 3, 5 and 7 are used for the analysis of equilibrium batch experiment data assuming the linear, Langmuir, and Freundlich isotherms, respectively. Figure 3 and Figure 4 present the adsorption isotherms for aqueous ion solutions corresponding to the fit of the Freundlich isotherm plots for Co^{2+}, Cu^{2+}, and Zn^{2+} adsorption on modified SBA-15.

Batch tests with Co^{2+}, Cu^{2+}, and Zn^{2+} in single solutions were used to estimate the quantity adsorbed by modified SBA-15. The equilibrium data were fitted very well to the Langmuir isotherm. Calculation of the isotherm parameters using these plots provided the data presented in Table 2.

The Langmuir and Freundlich equations are the most commonly models employed to describe the adsorption

process in heterogeneous systems. The Langmuir model assumes monolayer adsorption on the solid surface, while Freundlich model is empirical in nature. All the isotherms showed a sharp initial slope, indicating that the materials acted as high efficacy adsorbents at broad range of metal concentrations; in addition, when the aqueous metal concentration increased, the saturation constant value was reached. The equilibrium data were analyzed using regression analysis to fit the isotherm models (Figures 3 and 4) and the equation constants are tabulated in Table 2. The Langmuir model should better describe the adsorption system on modified SBA-15 than the Freundlich model. On the other hand, the values of n were all greater than 1 for the different materials, indicative of high adsorption intensity.

As shown in Figures 3 and 4, adsorption was greater for Zn^{2+} and Cu^{2+}, and the affinity of the modified SBA-15 adsorbents followed the common order Zn^{2+} > Cu^{2+} > Co^{2+}. The same order of affinity was found for the other SBA-15 materials (CY-SBA-15 and NH$_2$-SBA-15). As shown in Table 2, both modified materials showed greater adsorption for Zn^{2+} than the other metal ions. We can also say that the adsorption of all cations was very fast.
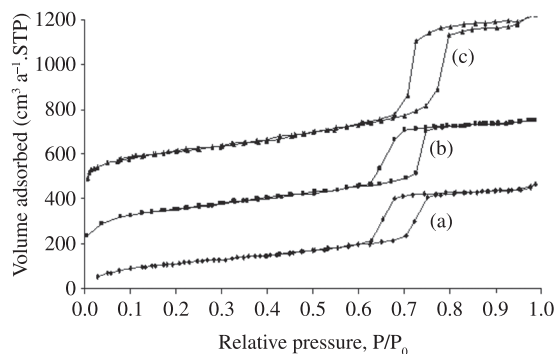

Figure 3. Adsorption isotherm from aqueous of modified SBA-15 for Co^{2+}, Cu^{2+}, and Zn^{2+}: Langmuir model.
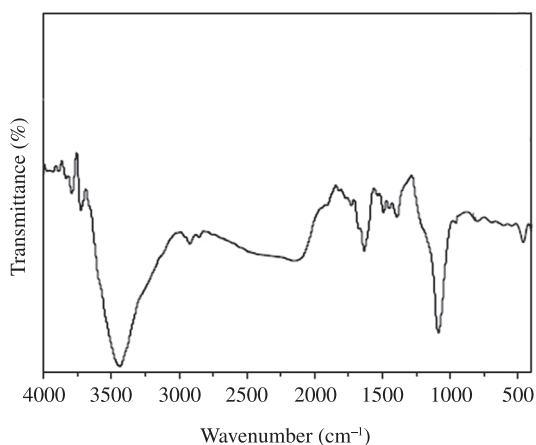
Figure 4. Adsorption isotherm from aqueous of modified SBA-15 for Co^{2+}, Cu^{2+}, and Zn^{2+}: Freundlich model.

3.3.3. Ion competitive adsorption studies.

The competitive adsorption of Cu^{2+}, Co^{2+}, and Zn^{2+} ions, was studied on CY-SBA-15 material that has highest adsorptivity for all the ions, that are summarized in Table 2. Both modified materials showed a higher adsorption capacity for Zn^{2+} than for the other metal ions; the affinity of the adsorbents for different ions decreased in the order: $Zn^{2+} > Cu^{2+} > Co^{2+}$. The complexation selectivity coefficients (K_F) of Zn^{2+} in the presence of other Me^{2+} ions ($Me^{2+} = Cu^{2+}$ and Co^{2+}) were calculated according to Equation 6) The K_F values obtained for the CY–SBA-15 adsorbent were 14.20, 11.14, and 7.56 for Zn^{2+}, Cu^{2+}, and Co^{2+}, respectively. These values were much higher than those obtained for the unmodified SBA-15 sample (1.31, 1.13, and 0.92 for Zn^{2+}, Cu^{2+}, and Co^{2+}, respectively), indicating that CYANEX 272 was highly and selectively complexed with Zn^{2+} ions. We considered that the adsorption mechanism of metal cations was different for the organically functionalized NH_2-SBA-15 and CY-SBA-15. In the first case, complexation is the major mechanism for metal ion adsorption. This mechanism is governed by the formation constants of the metal complexes and, consequently, the Q values are affected by the competition between different ions in solution and are limited by the amount of surface-grafted ligand. In contrast, the mechanism of cation adsorption onto amorphous functionalized silica is based not only on the complexation between the metal ion and the ligand, but a physisorption mechanism is also involved. In this case, the Q value increases when the total metal ion concentration increases.

Figures 5 and 6 present the adsorption isotherms for mixed aqueous ion solutions corresponding to the Langmuir and Freundlich isotherm plots of Co^{2+}, Cu^{2+}, and Zn^{2+} adsorption on CY-SBA-15, respectively. The equilibrium data were fitted very well to the Langmuir isotherm. Calculation of the isotherm parameters using these plots provided the data presented in Table 2. We observed the same affinity between metallic cations and the material as in single solute adsorption. The same observations were noted for NH_2-SBA-15 and unmodified SBA-15.

3.3.4. Immersion enthalpies

Figure 7 shows of the enthalpies as a function of the concentration of the studied ions. Calorimetric studies showed that the immersion of the different modified solids in the respective ion solutions generated values of enthalpy in the range between 20 J.g^{-1} and 140 J.g^{-1}. The figure shows behavior that is comparable to the isotherm of adsorption from an aqueous solution. This should be highlighted as an interesting aspect, since by using thermodynamics, it is possible to study the adsorption capacity of modified SBA.

The highest value of enthalpy was obtained for the immersion of CY-SBA-15 in the zinc ion solution, with the while the lowest value of immersion enthalpy was obtained for the immersion SBA-15 in the solution of cobalt. Enthalpy values were between –29 J.g^{-1} (Co^{2+}– SBA-15) and –140 J.g^{-1} (Zn^{2+}–CY–SBA-15), as shown in Figure 7. This

behavior agrees with textural characteristics of modified SBA-15 and the diameters of the ions under study. It should be noted that the behavior of immersion enthalpies of the solids synthesized in this work was very similar to the isotherm data.
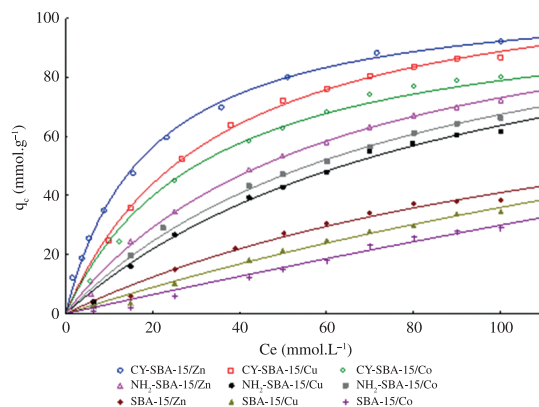

Figure 5. Adsorption isotherm for modified SBA-15 using mixed aqueous solutions of Co^{2+}, Cu^{2+} and Zn^{2+}: Langmuir model.
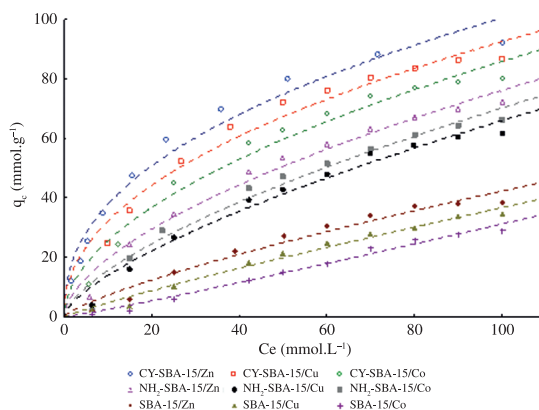

Figure 6. Adsorption isotherm for modified SBA-15 using mixed aqueous solutions of Co^{2+}, Cu^{2+} and Zn^{2+}: Freundlich model.
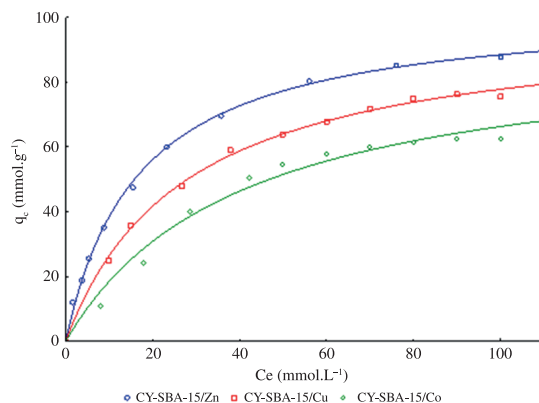

Figure 7. Immersion enthalpies of metallic ions in modified SBA-15.

4. Conclusions

An effective adsorbent for metal ions was prepared by the immobilization of 3-aminopropyl-triethoxysilane and bis(2,4,4-trimethylpentyl) phosphinic acid (Cyanex 272) groups on the surface of SBA-15 mesoporous silica. The high density of the organic groups grafted onto the SBA-15 surface resulted in remarkable adsorption capacities for Cu^{2+}, Co^{2+}, and Zn^{2+} ions. The hybrid material showed higher adsorption selectivity for Zn^{2+} compared to the other metal ions present in a mixed metal ion solution. These results suggest the possibility of employing this material in the selective recovery of the Zn^{2+} ions from a mixed metal ion solution. The technique of immersion calorimetry also allowed further evaluation of the synthesized solids, and is the novel contribution of this research. This was accomplished because this thermodynamics technique is very sensitive.

References

1. Occelli M and Robson H. *Synthesis Of Microporous Materials*: Expanded Clays and Other Microporous Solids. New York: Academic Press; 1992.

2. Barrer RM. *Zeolites and Clay Minerals as Sorbents and Molecular Sieves*. New York: Academic Press; 1978.

3. Jacobsen AJ. Intercalation Reactions of Layered Compounds. In: Cheetham AK and Day P, editors. *Solid State Chemistry Compounds*. Clarendon: Oxford; 1992. p. 182-233.

4. Clearfield A. Metal-phosphonate chemistry. *Progress in Inorganic Chemistry*. 1998; 47:371-510. http://dx.doi.org/10.1002/9780470166482.ch4

5. Alberti G, Costantino U. Two and three- dimensional Inorganic Networks. In: Atwood JL, Davies JED, MacNicol DD and Vogtle F, editors. *Comprehensive Supramolecular Chemistry*. New York: Elsevier Science; 1996.

6. Alberti G, Costantino U. Intercalation of zirconium phosphates and phosphonates. In: Atwood JL, Davies JED, MacNicol DD, editors. *Inclusion Compounds*. New York: Oxford University Press; 1991. p. 136.

7. Smith G, Cloutt BA, Lynch DE, Byriel KA, Kennard CHL. Nitrogen base adducts with silver(I) p-toluenesulfonate: syntheses and single crystal X-ray characterizations of the adducts with pyridine (1:1), 2-aminopyridine (1:2), 2-aminopyrimidine (1:1), 4,6-dimethyl-2-aminopyrimidine (2:3), and 3-aminobenzoic acid (1:2) and the crystal structure of the parent silver(I) *p*-toluenesulfonate. *Inorganic Chemistry*. 1998; 37(13):3236-3242. http://dx.doi.org/10.1021/ic9706461

8. Shimizu GKH, Enright GD, Ratcliffe CI, Rego GS, Reid JL and Ripmeester JA. Silver sulfonates: an unexplored class of layered solids. *Chemistry of Materials*. 1998; 10(11):3282-3283. http://dx.doi.org/10.1021/cm980409b

9. Dalrymple SA and Shimizu GKH. An open channel coordination framework sustained by cooperative primary and secondary sphere interactions. *Chemical Communications*. 2002; 19:2224-2225. http://dx.doi.org/10.1039/b205952e

10. Dalrymple SA and Shimizu GKH. Anion exchange in the channels of a robust alkaline earth sulfonate coordination network. *Chemistry*. 2002; 8(13):3010-3015. http://dx.doi.org/10.1002/1521-3765(20020703)8:13<3010::AID-CHEM3010>3.0.CO;2-5

11. Cote AP and Shimizu GKH. Coordination solids via assembly of adaptable components: systematic structural variation in alkaline earth organosulfonate networks. *Chemistry*. 2003; 9(21):5361-5370. http://dx.doi.org/10.1002/chem.200305102

12. Prior TJ, Bradshaw D, Teat SJ and Rosseinsky MJ. Designed layer assembly: a three-dimensional framework with 74% extra-framework volume by connection of infinite two-dimensional sheets. *Chemical Communications*. 2003; 4:500-501. http://dx.doi.org/10.1039/b211124c

13. Lu JY, Lawandy MA, Li J, Yuen T and Lin CL. A new type of two-dimensional metal coordination system: hydrothermal synthesis and properties of the first oxalate−bpy mixed-ligand framework $_{\infty}^{2}$ [M(ox)(bpy)] (M = Fe(II), Co(II), Ni(II), Zn(II); ox = $C_2O_4^{2-}$; bpy = 4,4'-bipyridine). *Inorganic Chemistry*. 1999; 38(11):2695-2704. http://dx.doi.org/10.1021/ic990243w

14. Munakata M, Liu SQ, Konaka H, Kuroda-Sowa T, Suenaga Y, Maekawa M et al. Syntheses, structures, and properties of intercalation compounds of silver(I) complex with [2.2] paracyclophane. *Inorganic Chemistry*. 2004; 43(2):633-641. http://dx.doi.org/10.1021/ic0302433

15. Shimizu GKH, Enright GD, Ratcliffe CI, Ripmeester JA and Wayner DDM. Self-assembly of lamellar and expanded lamellar coordination networks. *Angewandte Chemie International Edition*. 1998; 37(10):1407-1409. http://dx.doi.org/10.1002/(SICI)1521-3773(19980605)37:10<1407::AID-ANIE1407>3.0.CO;2-D

16. Holman KT, Pivovar AM, Swift JA and Ward MD. Metric engineering of soft molecular host frameworks. *Accounts of Chemical Research*. 2001; 34(2):107-108. http://dx.doi.org/10.1021/ar970272f

17. Holman KT, Pivovar AM and Ward MD. Engineering crystal symmetry and polar order in molecular host frameworks. *Science*. 2001; 294:1907-1911. http://dx.doi.org/10.1126/science.1064432

18. Uemura K, Kitagawa S, Fukui K and Saito K. A Contrivance for a dynamic porous framework: cooperative guest adsorption based on square grids connected by amide−amide hydrogen bonds. *Journal of the American Chemical Society*. 2004; 126(2):3817-3828. http://dx.doi.org/10.1021/ja039914m

19. Chen BL, Fronczek FR and Maverick AW. Solvent-dependent 4^4 square grid and $6^4.8^2$ NbO frameworks formed by Cu(Pyac)$_2$ (bis[3-(4-pyridyl)pentane-2,4-dionato]copper(II)). *Chemical Communications*. 2003; 17:2166-2167. http://dx.doi.org/10.1039/b305457h

20. Pschirer NG, Ciurtin DM, Smith MD, Bunz UHF and Hands-Conrad ZL. Noninterpenetrating square-grid coordination polymers with dimensions of 25×25 Å^2 prepared by using N,N'-type ligands: the first chiral square-grid coordination polymer. *Angewandte Chemie International Edition*. 2002; 41(4):583-585. http://dx.doi.org/10.1002/1521-3773(20020215)41:4<583::AID-ANIE583>3.0.CO;2-I

21. Biradha K, Hongo Y and Fujita M. Open square-grid coordination polymers of the dimensions 20×20 Å: remarkably stable and crystalline solids even after guest removal. *Angewandte Chemie International Edition*. 2000; 39(21):3843-3845. http://dx.doi.org/10.1002/1521-3773(20001103)39:21<3843::AID-ANIE3843>3.0.CO;2-#

22. Zaworotko MJ. Superstructural diversity in two dimensions: crystal engineering of laminated solids. *Chemical Communications*. 2001; 1:1-9. http://dx.doi.org/10.1039/b007127g

23. Zaporozhets O, Petruniock N, Bessarabova O and Sukhan V. Determination of Cu(II) and Zn(II) using silica gel loaded with 1-(2-thiasolylazo)-2-naphthol. 1999. *Talanta*. 1999; 49(4):899-906. http://dx.doi.org/10.1016/S0039-9140(99)00085-5

24. Soliman E, Mahmoud M and Ahmed S. Synthesis, characterization and structure effects on selectivity properties of silica gel covalently bonded diethylenetriamine mono- and bis-salicylaldehyde and naphthaldehyde Schiff's bases towards some heavy metal ions. *Talanta*. 2001; 54(2):243-248. http://dx.doi.org/10.1016/S0039-9140(00)00648-2

25. Yamini Y, Hassan J, Mohandesi R and Bahramifar N. Preconcentration of trace amounts of beryllium in water samples on octadecyl silica cartridges modified by quinalizarine and its determination with atomic absorption spectrometry. *Talanta*. 2002; 56(3):375-381. http://dx.doi.org/10.1016/S0039-9140(01)00560-4

26. Abou-El-Sherbini Kh, Kenawy IMM, Hamed MA, Issa RM and Elmorsi R. Separation and preconcentration in a batch mode of Cd(II), Cr(III, VI), Cu(II), Mn(II, VII) and Pb(II) by solid-phase extraction by using of silica modified with N-propylsalicylaldimine. *Talanta*. 2002; 58(2):289-300. http://dx.doi.org/10.1016/S0039-9140(02)00248-5

27. Kresge CT, Leonowicz ME, Roth WJ, Vartulli JC and Beck JS. Ordered mesoporous molecular sieves synthesized by a liquid-crystal template mechanism. *Nature*. 1992; 359:710-712. http://dx.doi.org/10.1038/359710a0

28. Lee H, Yi J. Removal of copper ions using functionalized mesoporous silica in aqueous solution. *Separation Science and Technology*. 2001; 36 (11):2433-2448. http://dx.doi.org/10.1081/SS-100106101

29. Antoschuk V and Jaroniec M. 1-Allyl-3-propylthiourea modified mesoporous silica for mercury removal. *Chemical Communications*. 2002; 3:258-259. http://dx.doi.org/10.1039/b108789d

30. Babel S and Kurniawan TA. Low-cost adsorbent for heavy metals uptake from contaminated water: a review. *Journal Hazardous Materials*. 2003; 97(1-3):219-243. http://dx.doi.org/10.1016/S0304-3894(02)00263-7

31. Hossain KZ and Mercier L. Intraframework metal ion adsorption in ligand functionalized mesoporous silica. *Advanced Materials*. 2002; 14(15):1053-1056. http://dx.doi.org/10.1002/1521-4095(20020805)14:15<1053::AID-ADMA1053>3.0.CO;2-X

32. Walkarius A and Delacote C. Rate of access to the binding sites in organically modified silicates. 3. Effect of structure and density of functional groups in mesoporous solids obtained by the co-condensation route. *Chemistry of Materials*. 2003; 15(22):4181-4192. http://dx.doi.org/10.1021/cm031089l

33. Yoshitake H, Yakoi T and Tatsumi T. Adsorption of chromate and arsenate by amino-functionalized MCM-41 and SBA-1. *Chemistry of Materials*. 2002; 14(11):4603-4610. http://dx.doi.org/10.1021/cm0202355

34. Yee Ho K, McKay G and Lun Yeung K. Selective adsorbents from ordered mesoporous silica. *Langmuir*. 2003; 19(7):3019-3024. http://dx.doi.org/10.1021/la0267084

35. Zhang L, Yu C, Zhao W, Chen H, Li L and Shi J. Preparation of multi-amine grafted mesoporous silicas and their application to heavy metal ions adsorption. *Journal of Non-Crystalline Solids*. 2007; 353(44-46):4055-4061. http://dx.doi.org/10.1016/j.jnoncrysol.2007.06.018

36. Yang H, Xu R, Xue X, Li F and Li G. Hybrid surfactant-templated mesoporous silica formed in ethanol and its application for heavy metal removal. *Journal Hazardous Materials*. 2008; 152(2):690-698. http://dx.doi.org/10.1016/j.jhazmat.2007.07.060

37. Liu AM, Hidajat S and Zhao DY. A new class of hybrid mesoporous materials with functionalized organic monolayers for selective adsorption of heavy metal ions. *Chemical Communications*. 2000; 13:1145-1146. http://dx.doi.org/10.1039/b002661l

38. Walkarius A, Etienne M and Bessiere J. Rate of access to the binding sites in organically modified silicates. 1. Amorphous silica gels grafted with amine or thiol groups. *Chemistry of Materials*. 2002; 14(6):2757-2766. http://dx.doi.org/10.1021/cm021117k

39. Landau MV, Varkey SP, Herskowitz M, Regev O, Pevzner S, Sen T et al. Wetting stability of Si-MCM-41 mesoporous material in neutral, acidic and basic aqueous solutions. *Microporous and Mesoporous Materials*. 1999; 33(1-3):149-163. http://dx.doi.org/10.1016/S1387-1811(99)00133-X

40. De Clercq B, Lefebvre F and Verpoort F. Immobilisation of multifunctional Schiff base containing ruthenium complexes on MCM-41. *Applied Catalysis A*: General. 2003; 247(2):345-364. http://dx.doi.org/10.1016/S0926-860X(03)00126-1

41. Zhao D, Feng J, Huo Q, Melosh N, Fredrickson GH, Chmelka BF et al. Triblock copolymer syntheses of mesoporous silica with periodic 50 to 300 Angstrom pores. *Science*. 1998; 23:548-552. http://dx.doi.org/10.1126/science.279.5350.548

42. Khodakov AY, Zholobenko VL, Bechara R and Durand D. Impact of aqueous impregnation on the long-range ordering and mesoporous structure of cobalt containing MCM-41 and SBA-15 materials. *Microporous and Mesoporous Materials*. 2005; 79 (1-3):29-39. http://dx.doi.org/10.1016/j.micromeso.2004.10.013

43. Kang T, Park Y and Yi J. Highly selective adsorption of Pt2+ and Pd2+ using thiol functionalized mesoporous silica. *Industrial & Engineering Chemistry Research*. 2004; 43 (6):1478-1484. http://dx.doi.org/10.1021/ie030590k

44. Perez-Quintanilla D, Del Hierro I, Fajardo M and Sierra I. Mesoporous silica functionalized with 2-mercaptopyridine: synthesis, characterization and employment for Hg(II) adsorption. *Microporous and Mesoporous Materials*. 2006; 89(1-3):58-68. http://dx.doi.org/10.1016/j.micromeso.2005.10.012

45. Li J, Qi T, Wang L, Liu C and Zhang Y. Synthesis and characterization of imidazole-functionalized SBA-15 as an adsorbent of hexavalent chromium. *Materials Letters*. 2007; 61(14-15):3197-3200. http://dx.doi.org/10.1016/j.matlet.2006.11.079

46. Wang X, Lin KSK, Chan JCC and Cheng S. Direct synthesis and catalytic applications of ordered large pore aminopropyl-functionalized SBA-15 mesoporous materials. *Journal of Physical Chemistry B*. 2005; 109(5):1763-1769. http://dx.doi.org/10.1021/jp045798d

47. Wang L, Qi T and Zhang Y. Novel organic-inorganic hybrid mesoporous materials for boron adsorption. *Colloids and Surfaces A*: Physicochemical and Engineering

Aspects. 2006; 275(1-3):73-78. http://dx.doi.org/10.1016/j.colsurfa.2005.06.075

48. Gao Z, Wang L, Qi T, Chu J and Zhang Y. Synthesis, characterization, and cadmium(II) uptake of iminodiacetic acid-modified mesoporous SBA-15. *Colloids and Surfaces A:* Physicochemical and Engineering Aspects. 2007; 304(1-3):77-81. http://dx.doi.org/10.1016/j.colsurfa.2007.04.045

49. Abdel-Latif SA, Hassib HB and Issa YM. Studies on some salicylaldehyde Schiff base derivatives and their complexes with Cr(III), Mn(II), Fe(II), Ni(II) and Cu(II). *Spectrochimica Acta Part A*: Molecular and Biomolecular Spectroscopy. 2007; 67(3-4):950-957. http://dx.doi.org/10.1016/j.saa.2006.09.013

50. Brunel D, Cauvel A, Fajula F and Di Renzo F. MCM-41 type silicas as supports for immobilized catalysts. *Studies in Surface Science and Catalysis*. 1995; 97, 173-180. http://dx.doi.org/10.1016/S0167-2991(06)81887-2

51. Martin T, Galarneau A, Brunel D, Izard V, Hulea V, Blanc AC et al. Towards total hydrophobisation of MCM-41 type silica surface. *Studies in Surface Science and Catalysis*. 1995; 135:178. http://dx.doi.org/10.1016/S0167-2991(01)81330-6

52. Giraldo L, Cubillos GI and Moreno JC. Evaluación de las pérdidas térmicas en calorimetría isoperibólica. Importancia de los alrededores en la obtención de constantes instrumentales. *Revista Colombiana de Química*. 2005; 34:147-154.

53. Palkovits R, Yang CM, Olejnik S and Schüth F. Active sites on SBA-15 in the Beckmann rearrangement of cyclohexanone oxime to e-caprolactam. *Journal of Catalysis*. 2006; 243(1):93-98. http://dx.doi.org/10.1016/j.jcat.2006.07.004

54. Mihaela M, Reiss A, Stefanescu I, David E, Parvulescu V and Renard G. Modified SBA-15 mesoporous silica for heavy metal ions remediation. *Chemosphere*. 2008; 73(9):93-98:1499-1504.

55. Jiang Y, Gao Q, Yu H, Chen Y and Deng F. Intensively competitive adsorption for heavy metal ions by PAMAM-SBA-15 and EDTA-PAMAM-SBA-15 inorganic-organic hybrid materials. *Microporous and Mesoporous Materials*. 2007; 103(1-3):316-324. http://dx.doi.org/10.1016/j.micromeso.2007.02.024

56. Zhao D, Huo Q, Feng J, Chmelka BF and Stucky GD. Nonionic triblock and star diblock copolymer and oligomeric surfactant syntheses of highly ordered, hydrothermally stable, mesoporous silica structures. *Journal of the American Chemical Society*. 1998; 120(24):6024-6036. http://dx.doi.org/10.1021/ja974025i

57. Girish Kumar K and Saji John K. Complexation and ion removal studies of a polystyrene anchored Schiff base. *Reactive and Functional Polymers*. 2006; 66(12):1427-1433. http://dx.doi.org/10.1016/j.reactfunctpolym.2006.04.006

58. Refat MS, El-Deen IM, Ibrahim HK and El-Ghool S. Synthesis and spectroscopic studies of some transition metal complexes of a novel Schiff base ligands derived from 5-phenylazo-salicylaldehyde and o-amino benzoic acid. *Spectrochimica Acta Part A: Molecular and Biomolecular Spectroscopy*. 2006; 65(5):1208-1220. http://dx.doi.org/10.1016/j.saa.2006.01.049

59. Shriver DF, Atkins PW and Langford CH. *Inorganic Chemistry*. Oxford: University Press Oxford; 1992.